Compositional dependence of the giant magnoresistance in FexRh1-x thin films

Compositional dependence of the giant magnetoresistance in Fe_xRh_{1-x} thin films

J. van Driel[a)]
Van der Waals-Zeeman Institute, University of Amsterdam, Valckenierstraat 65, 1018 XE Amsterdam, The Netherlands

R. Coehoorn
Philips Research Laboratories, Prof. Holstlaan 4, 5656 AA Eindhoven, The Netherlands

G. J. Strijkers
Department of Physics and COBRA, Eindhoven University of Technology, P.O. Box 513, 5600 MB Eindhoven, The Netherlands

E. Brück and F. R. de Boer
Van der Waals-Zeeman Institute, University of Amsterdam, Valckenierstraat 65, 1018 XE Amsterdam, The Netherlands

(Received 31 July 1998; accepted for publication 8 October 1998)

In this article we report on the magnetic and transport properties of Fe_xRh_{1-x} thin films, prepared by evaporation in high vacuum, in the composition range $0.41<x_{Fe}<0.59$. Upon annealing (at a temperature of 870 K or higher) a certain volume fraction transforms to the ordered CsCl-type (α') FeRh phase. Close to room temperature this phase shows a hysteretic transition between the antiferromagnetic (AF) and the ferromagnetic (F) state for samples with $x_{Fe}<0.5$, which gives rise to a magnetoresistance (MR) effect. Although the magnetic transition was never found to be complete, it is shown that the full MR ratio can be obtained by extrapolation of the measured MR ratio as a function of the relative change of the magnetization at the transition. The AF→F transition is only observed for films with $x_{Fe}<0.505\pm0.015$, for which the α' phase with this (fixed) composition is present together with a nonmagnetic Rh-rich fcc-type phase, as is shown from a combination of x-ray diffraction, Mössbauer spectroscopy, and magnetization studies. This observation, which was not expected from the phase diagrams available from the literature, can explain our finding that the full MR ratio observed for films in this compositional range is independent of the Fe content. The full MR ratio is $85\pm6\%$ at room temperature, which is very close to the MR ratio observed for bulk FeRh, implying a high structural quality of the films grown. X-ray diffraction and transmission electron microscopy were used to quantify microstructural aspects such as the grain diameter and strain. The highest MR ratio actually observed is 58%, in a 4400 kA/m field at 275 K. The full MR increases to approximately 150% at 250 K, and, as estimated from the resistivity of F and predominantly AF samples with almost the same composition, to $680\pm100\%$ at 4.2 K. © *1999 American Institute of Physics.* [S0021-8979(99)01802-2]

I. INTRODUCTION

Giant magnetoresistance (GMR) in multilayers and spin valves has received a great deal of attention after the discovery of the effect in 1988.[1] However, artificially layered structures are not the only materials to show these large magnetoresistance (MR) effects, certain intermetallic compounds can also show a considerable MR effect.[2] In this article we focus on the intermetallic compound Fe–Rh. As early as 1974 Schinkel *et al.*[3] measured a MR ratio of approximately 1700% at 4.2 K for polycrystalline bulk $Fe_{0.505}Rh_{0.495}$, and Algarabel *et al.*[4] found for bulk $Fe_{0.5}Rh_{0.5}$ a MR ratio of $\pm90\%$ at room temperature. The change in the resistance is linked to the transition of the compound from the low-temperature antiferromagnetic (AF) to the high-temperature ferromagnetic (F) state. For stochiometric FeRh at zero applied field and at zero pressure, this transition takes place at $T_{F-AF}=405$ K.[5] A large number of articles have been published treating the magnetic transition of bulk Fe–Rh as a function of either temperature[6] or magnetic field[7,8] and dealing with its dependence on composition,[9] heat treatment,[10,11] and pressure.[12,13] The magnetic transition is accompanied by a change of the lattice parameters[14] and the elastic[5,15] and electrical transport[3,4] properties.

According to the phase diagram[16] shown in Fig. 1, at room temperature Fe_xRh_{1-x} compounds have the CsCl-type structure (α' phase) for $x_{Fe}>0.485$. For $0.33<x_{Fe}<0.485$ there is a two-phase region where both the α' phase and γ phase (fcc solid solution of Fe and Rh) are present. In compounds containing between 33 and 55 at. % Fe the α' phase shows a transformation between the low-temperature AF state and the high-temperature F state. At high temperatures, about 1600 K for $x_{Fe}=0.5$ and 900 K for $x_{Fe}=0.8$, there is a

[a)]Present address: Philips Research Laboratories, Postbox WA03, Prof. Holstlaan 4, 5656 AA Eindhoven, The Netherlands; electronic mail: drieljv@natlab.research.philips.com

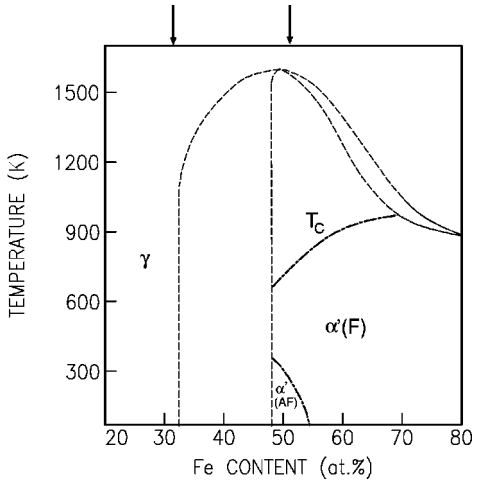

FIG. 1. Phase diagram for Fe–Rh compound as given by Kubaschewski (Ref. 16). Lines separating single phase and two-phase regions are indicated with dashed lines. Magnetic transition temperatures are indicated with a dashed-dotted line. As discussed in Sec. IV A, the two arrows in the upper part of the figure indicate the boundaries between the single phase and two-phase regions as observed in our thin films.

phase transition from the α' phase to the γ phase. Swartzendruber[17] has proposed a similar phase diagram, but with the boundary between the α' and the α'/γ two-phase region shifted to $x_{\mathrm{Fe}}=0.47$ at room temperature.

Neutron diffraction experiments[18–20] indicate that in the AF α' phase each Fe atom is surrounded by 6 Fe atoms with opposite spin direction. For an equiatomic FeRh compound the magnetic moments of the Fe and Rh atoms are 3.3 and $0\,\mu_B$ in the AF state, and in the F state they are 3.1 and $1.0\,\mu_B$, respectively. Values of magnetic moments for Fe and Rh atoms obtained from self-consistent total-energy calculations[21,22] show a good agreement with these experimental results. Mössbauer spectroscopy[23] indicates that excess Fe atoms are positioned on Rh sites in the lattice, having a lower magnetic moment than Fe atoms on Fe sites.

Although the transport and magnetic properties of bulk Fe–Rh are well known today, less research has been done on thin films. Lommel observed the AF→F phase transition in Fe–Rh thin films that were obtained by annealing Fe–Rh multilayers deposited by evaporation.[24] Whereas the temperature hysteresis of the transition is only of the order 10 K for bulk samples, he found a hysteresis of the order of 100 K for the thin films. The saturation magnetization above the transition temperature was observed to be only half of that of the bulk material, whereas well below the transition temperature part of the magnetization was found to be retained, suggesting that at all temperatures the films consisted of a mixture of AF and F phases. The AF→F transition was observed to be accompanied by a decrease of the resistance of approximately 40%, less than half the value (±90%) reported in the bulk material.[4] Recently Ohtani and Hatakeyama observed a similarly large thermal hysteresis of the magnetic transition in sputter deposited Fe–Rh films, and concluded from intensive structural investigations that it is related to the presence of a secondary fcc (γ) phase and to compositional fluctuations.[25] In a second publication the same authors showed that stress in the films, and the stress distribution, strongly affect the magnetic transition temperature and the hysteresis and steepness of the transition.[26] No data on the magnetoresistance are given in Refs. 25 and 26.

In this article we report on a study of the magnetoresistance of $\mathrm{Fe}_x\mathrm{Rh}_{1-x}$ thin films close to the equiatomic composition, prepared by coevaporation of Fe and Rh and subsequent annealing. The purpose of our study was to establish the relationship between the film composition and the degree of completeness of the magnetic transition on the one hand, and the magnetoresistance on the other hand. This is one of the issues that is of interest when assessing the suitability of Fe–Rh films for applications in magnetic field sensors. Our experimental results support the earlier finding of an MR ratio that is less than the bulk value. In principle, this could be the result of structural differences in the F or AF phases as compared to the bulk compound (e.g., a difference in the degree of site disorder, or a different scattering rate at grain boundaries), leading to a difference in the spin dependence of scattering or in the spin flip scattering rate. However, we show that the effect is fully consistent with a model within which the MR ratio for films with different Fe content is proportional to the ratio of the magnetization change upon the magnetic transition. We will show that data taken at different alloy compositions extrapolate to the same (full) MR ratio, which is found to be essentially the same as that for bulk FeRh. This can be explained from the fact that the composition of the α' phase in the films responsible for the AF→F transition, is the same in all cases, $x_{\mathrm{Fe}}=0.505\pm0.015$. Films with a larger Fe content do not show the AF→F transition. Films with $0.43<x_{\mathrm{Fe}}<0.505$ consist of a two-phase mixture of γ and α' phases with the composition mentioned. This result was unexpected, as bulk phase diagrams suggest a single α' phase showing the AF→F transition for approximately $0.485<x_{\mathrm{Fe}}<0.55$.[10,16,17]

In Sec. II we give an overview of the experimental procedure for fabrication and characterization of the thin films. In Sec. III we will present the results obtained using several characterization techniques after different annealing treatments and the results of magnetization and magnetoresistance measurements. The influence of the microstructure and composition of the films on the magnetic and electrical transport properties will be discussed in Sec. IV, in which an estimate of the full MR ratio is given. Finally, we will present a summary and conclusions in Sec. V.

II. EXPERIMENTAL PROCEDURE

The films were fabricated by coevaporation of Fe and Rh onto fused quartz substrates in a HV evaporation chamber with a background pressure of 10^{-6} Pa and a deposition rate of 0.5 nm/s. Deposition took place at room temperature or at 520 K. The substrates were mechanically polished before deposition, no predeposition cleaning (sputter-etch, chemical cleaning) was administered. The total thickness of the films was 100 nm. The composition of the films was determined

using Rutherford backscattering spectroscopy (RBS). The Fe contents of the samples ranged between 41 and 59 at. %, with an accuracy of ± 0.5 at. %.

To obtain the ordered α' crystal structure from the as-deposited disordered structures, several annealing procedures were used during which the crystallographic transitions were monitored. The resistance of the films was measured during annealing in vacuum ($p < 10^{-4}$ Pa). When annealing in a Faraday balance the magnetization could be measured during the procedure, with the sample placed in a magnetic field of 400 kA/m and in a He-atmosphere. For all procedures the heating rate was 10 K/min. The maximum temperature was maintained from 1 min up to 16 h. The maximum temperatures used were 970 K or lower.

The films were characterized using x-ray diffraction (XRD), scanning electron microscopy (SEM), and transmission electron microscopy (TEM). The amounts of the various crystallographically and magnetically distinct phases in the films were determined using ^{57}Fe conversion electron Mössbauer spectroscopy with a source of ^{57}Co in a Rh matrix.

A Faraday balance and a superconducting quantum interference device (SQUID) magnetometer were used to measure the magnetization as a function of temperature and magnetic field. The resistivity as a function of temperature and magnetic field was measured using a four-point probe method.

III. RESULTS

A. Crystal and grain structure before and after the annealing treatment

The as-deposited Fe_xRh_{1-x} films have a disordered γ phase structure for $x_{Fe} < 0.55$ and consist of a mixture of disordered bcc (α) and fcc (γ) phases for $x_{Fe} > 0.55$. The disordered α phase is not present in bulk materials of this composition. The α phase is ferromagnetic at room temperature and the γ phase is paramagnetic.

Figure 2 shows the magnetization (a) and the relative resistance (b) measured during the annealing procedure for two samples with 49.0 at. % Fe. When the film is heated there is an upturn in the resistance curve at about 550 K and at the same temperature a finite magnetization develops. XRD shows a change from the disordered γ to the disordered α phase. This crystallographic transition seems to be of a martensitic character, i.e., diffusionless. For films with less than 51 at. % Fe this transition is not complete, i.e., there is some retained γ phase even after annealing at 970 K for 16 h. The temperature at which the $\gamma \rightarrow \alpha$ transition takes place increases with increasing Rh content. At still higher temperatures the α phase gradually transforms into the ordered α' phase, as is evidenced by the appearance of an (100) superlattice peak in the XRD spectrum. Annealing temperatures of 870 K or higher are needed to have a largely ordered crystal structure. In a film with $x_{Fe} < 0.5$, the α' phase becomes antiferromagnetic at low temperatures. For $x_{Fe} = 0.49$ the F→AF transition sets in at 300 K and is completed around 80 K.

SEM shows that there is considerable grain growth during annealing. For all compositions the as-deposited films

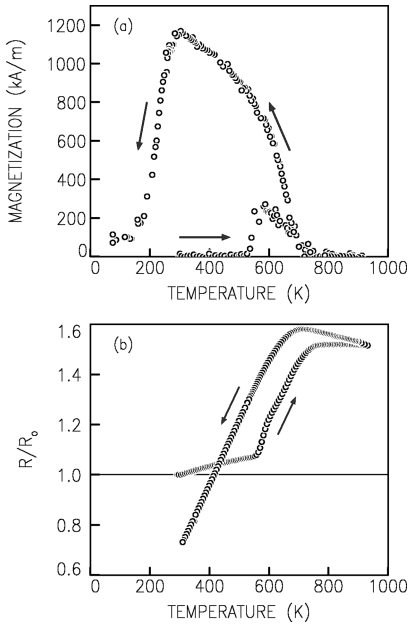

FIG. 2. Magnetization (a) and relative resistance (b) during the anneal procedure for two different samples with 49.0 at. % Fe. The arrows show the direction of the temperature cycle.

have grain sizes $\leqslant 10$ nm. After annealing at 970 K for 4 h, samples with 50.9 at. % Fe and 58.8 at. % Fe had average grain sizes of 80 and 130 nm, respectively (Fig. 3). The observation of an increase of the average grain size with Fe content is qualitatively consistent with the analysis of Ohtani and Hatakeyama[25] for 200 nm-thick sputter-deposited films, but the increase in grain size they observe (from 30 nm at 46.0 at. % Fe to 400 nm at 54.6 at. % Fe after annealing at

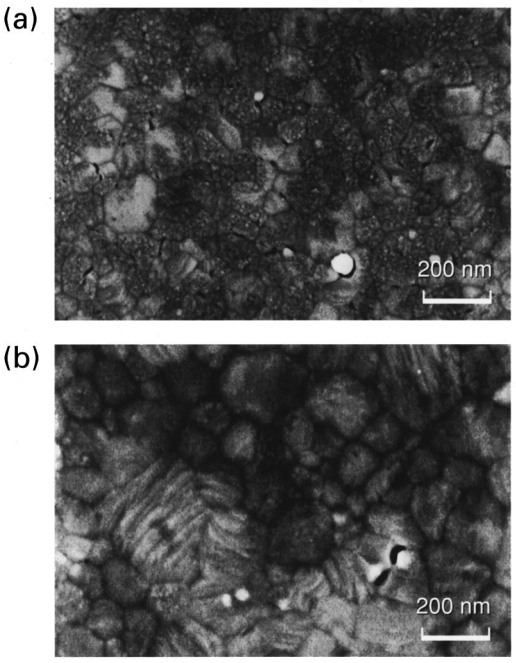

FIG. 3. SEM surface images for two samples with $x_{Fe} = 0.509$ (a) and $x_{Fe} = 0.588$ (b) after annealing at 970 K for 4 h.

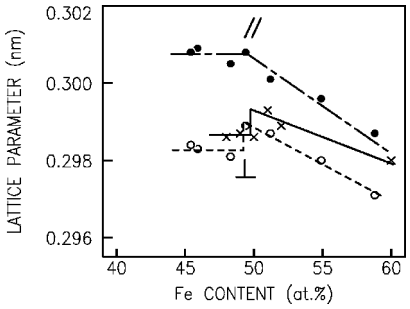

FIG. 4. Compositional dependence of the perpendicular-to-plane (open circles) and in-plane (closed circles) lattice parameter of thin films at room temperature compared with the bulk lattice parameters (Ref. 23) (crosses). The dashed lines are only guides-to-the-eye.

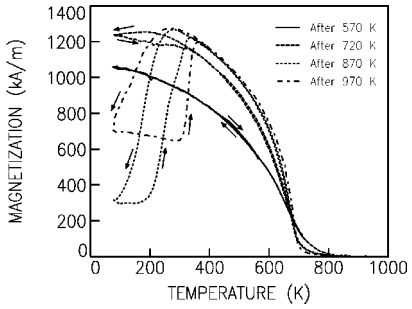

FIG. 5. Magnetization as a function of temperature for a sample with 49.2 at. % Fe during subsequent heating to 570, 720, 870, and 970 K. Between each heating cycle the sample is cooled down to 77 K and then heated to the next temperature, all in a magnetic field of 400 kA/m. The arrows give the direction of the temperature cycles.

870 K) is much larger than in our case, which could be due to the difference in deposition techniques.

XRD has been used to determine the lattice parameters of the α' phase, both perpendicular and parallel to the plane of the film (Fig. 4). All measurements were performed at room temperature. The samples with $x_{Fe}>0.49$ were in the ferromagnetic state. The samples with $x_{Fe}<0.49$ were measured after cooling to 4.2 K and subsequent heating to room temperature, which results in predominantly antiferromagnetic ordering. However, a considerable part of the α' phase is still ferromagnetic (as will be explained later in part B of this section). It is reported that in bulk Fe–Rh samples there is a 0.3% increase in lattice parameter at the AF→F transition.[7,14] For our thin films only a single spectrum is visible. We note that the difference between the peak positions of the two spectra is insufficient, with respect to the broadness of the peaks, to be resolved. This is caused by the small grain sizes in our thin films.

The in-plane lattice parameter was found to be larger than the perpendicular-to-plane lattice parameter. For films with $x_{Fe}<0.49$ the difference is 0.8% and it decreases to 0.6% for $x_{Fe}=0.588$, indicating a considerable tensile stress in the film. We will discuss the implications of this stress for the magnetic transition later in Sec. IV D. Figure 4 also includes the bulk lattice parameters as reported in the literature.[23] For $x_{Fe}<0.5$ the bulk lattice parameter is for completely AF samples.

B. Influence of annealing temperature and time on the magnetic properties

Samples were annealed for different times at several temperatures to investigate the influence of the annealing procedure on the magnetic and transport behavior. Figure 5 shows the magnetization as a function of temperature for a sample with 49.2 at. % Fe during heating to 570, 720, 870, and 970 K. The highest temperature in each case was maintained for no longer than 1 min and the cooling and heating rate were both approximately 10 K/min. Between each temperature cycle the sample is cooled down to 77 K and then heated to the next temperature, all in a magnetic field of 400 kA/m.

After heating to 570 K the sample is ferromagnetic at all temperatures, indicating the presence of disordered α phase. After heating to 720 K a weak F→AF transition is visible upon cooling and the magnetization has increased indicating a start of the formation of the α' phase. After heating to 870 K the amount of α' phase has increased resulting in a higher saturation magnetization and a more pronounced magnetic transition. Heating to 970 K does not increase the magnetization, but the hysteresis of the magnetic transition has become larger, so large that a significant part of the sample remains ferromagnetic even when approaching 0 K. The transition temperature for the AF→F transition, defined as the temperature at which the change of the magnetization with temperature shows a maximum, as measured upon increasing temperature, becomes higher. We have compared the transition temperatures for samples in the range $0.41<x_{Fe}<0.49$ after annealing at 920 and 970 K. After annealing at 970 K the average transition temperature is 340 ± 10 K, whereas after annealing at 920 K the observed transition temperatures fall in the range 270-340 K. After annealing at 720 K, other annealing steps no longer have an influence on the Curie temperature of the samples. An average Curie temperature of 695 ± 8 K is found for samples in the range $0.4<x_{Fe}<0.5$. For samples with excess Fe the Curie temperature increases with increasing Fe content, to $T_C=860$ K for $x_{Fe}=0.55$.

The time during which the maximum temperature was maintained, ranged between 1 min and 16 h. No influence of annealing time on the magnetic behavior was observed and also XRD did not show a distinct change in microstructure.

C. Mössbauer spectroscopy

^{57}Fe-Mössbauer spectroscopy can be used to identify and quantify the presence of magnetically and crystallographically distinct phases in the films. Shirane *et al.*[23] have performed extensive Mössbauer spectroscopy on Fe–Rh bulk samples with different compositions. They observed two distinct hyperfine fields for samples with $0.5<x_{Fe}<0.8$, corresponding to Fe atoms on Fe sites and on Rh sites in the lattice. The latter have a lower magnetic moment, but a higher hyperfine field. It is also possible to distinguish the AF and F phases on the basis of hyperfine spectra. More recently Ohtani and Hatakeyama[25] have performed Mössbauer spectroscopy on sputter-deposited Fe–Rh thin films in the composition range $0.46<x_{Fe}<0.55$. They find different

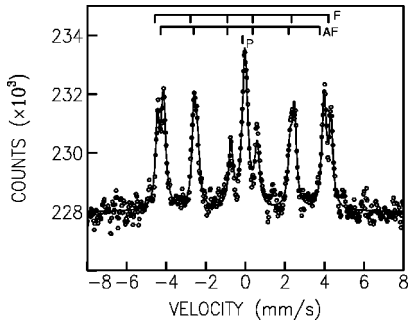

FIG. 6. Mössbauer spectrum for a film with 45.4 at. % Fe, heated to room temperature after cooling down to 4.2 K, showing two sextets for the α'(AF) and α'(F) phases and a singlet for the paramagnetic γ phase.

sextets, which are assigned to Fe atoms with 0, 2–6, and 8 Fe nearest neighbors in the α' phase. They also find two nonmagnetic γ phases.

We have performed ^{57}Fe-Mössbauer spectroscopy on our films at room temperature, after cooling to 4.2 K and after heating to 420 K, respectively. The films with $x_{Fe}<0.5$ have been investigated with predominantly AF ordering, as well as with predominantly F ordering. This was done by making use of the hysteresis in the AF-F magnetic transition with increasing and decreasing temperature. Figure 6 shows the spectrum for a film containing 45.4 at. % Fe which has been heated to room temperature after cooling down to 4.2 K. There are two sextets and a singlet present in the spectrum. Using the results reported by Shirane *et al.*[23] these can be identified. The singlet belongs to the paramagnetic γ phase. The two sextets belong to the AF and F phases with hyperfine fields of 25.4 and 27.5 T, respectively.

The amounts of γ, α'(AF) and α'(F) phases are obtained from the ratios between the intensities of the singlet and the two sextets. The magnetization direction in the film can be determined from the ratios of the intensities of the peaks of a sextet. The ratio is $3{:}\xi{:}1{:}1{:}\xi{:}3$, with $\xi=4$, 0, or 2 for an in-plane, perpendicular, or random magnetization direction. For the film in Fig. 6, we find $\xi=3.3$ for the F sextet and $\xi=1.6$ for the AF sextet, indicating that the magnetization is mostly in the plane of the film for the F phase and random for the AF phase.

When the Mössbauer spectrum of the same sample is measured after cooling down from 420 K to room temperature, only the paramagnetic singlet and the sextet belonging to the F phase are found. This implies that at a temperature of 420 K the AF→F transition is complete and that the F→AF transition starts at a temperature below room temperature. This is in agreement with the results from magnetization measurements of the same sample.

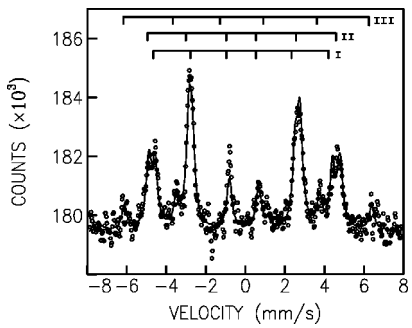

FIG. 7. Mössbauer spectrum for a film with 58.8 at. % Fe, showing three sextets corresponding to Fe atoms with 0–1, 2–3, and 8 Fe nearest neighbors.

TABLE I. Results of Mössbauer spectroscopy on films with $x_{Fe}<0.5$.

Fe content (at. %)	Amount of α' (AF) phase (%)	Amount of α' (F) phase (%)	Amount of γ (P) phase (%)	Temperature history
45.4	44.2	36.3	19.5	4.2 K, heating
	0	80.2	19.8	420 K, cooling
45.4	67.4	15.4	17.2	4.2 K, heating
45.9	54.6	28.8	16.6	4.2 K, heating
	0	82.4	17.6	420 K, cooling
48.3	84.5	0	15.5	4.2 K, heating
	56.6	30.5	12.9	420 K, cooling
49.0	44.0	47.9	8.1	4.2 K, heating
	0	87	13	420 K, cooling

All samples with $x_{Fe}<0.5$ show the same set of subspectra as the film with $x_{Fe}=0.454$ (shown in Fig. 6). The results of the fits are summarized in Table I, where the amounts of the respective phases are given. We have measured average hyperfine fields of 25.3 and 27.3 T and isomer shifts of 0.012 and 0.035 mm/s for the AF and F phases, respectively. These values do not change significantly with Fe content. There was no sextet belonging to Fe atoms on Rh sites visible in any of the samples measured, therefore we conclude that not more than a few percent of the Fe atoms occupy such sites. The amount of disorder in these films is therefore very small.

Samples with $x_{Fe}>0.5$ are always ferromagnetic, so a heat treatment before the measurements as described above does not affect the Mössbauer spectrum. The spectrum of a sample containing 58.8 at. % Fe is shown in Fig. 7. Three different sextets (I, II, and III) can now be distinguished. The hyperfine fields are listed in Table II. Making use of the analysis of the hyperfine field distribution in Fe-rich bulk compounds, as given by Shirane *et al.*,[23] we arrive at the following assignment of local environments to the Fe atoms giving rise to these three sextets. Sextets I and II result from Fe atoms on Fe sites, with between 0–1 and 2–3 Fe nearest neighbors, respectively. Sextet III is related to Fe atoms positioned on the Rh sites of the lattice (with 8 Fe nearest

TABLE II. Results of Mössbauer spectroscopy on films with $x_{Fe}>0.5$.

Fe content (at. %)	Subspectrum	B_{hf} (T)	Amount (%)	Description
51.2	I	27.2	99.3	0 nn. Fe
	IV	0	0.7	paramagnetic γ phase
54.9	I	27.8	100	0–1 nn. Fe
58.8	I	28.6	32.5	0–1 nn. Fe
	II	30.8	53.3	2–3 nn. Fe
	III	39.9	14.2	8 nn. Fe

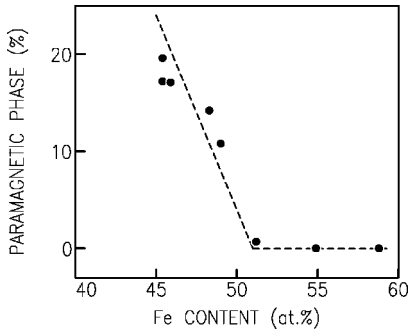

FIG. 8. Compositional dependence of the amount of paramagnetic γ phase determined from Mössbauer spectroscopy. The dashed line is a guide-to-the-eye.

neighbors). The excess amount of 8.8 at. % Fe in this sample should result in 15% of the total amount of Fe atoms being positioned on a Rh site. This compares well with the experimental value of 14%.

Two other samples with $x_{\mathrm{Fe}}>0.5$ have been investigated; the results are summarized in Table II. The film with 51.2 at. % Fe still contains a small amount of γ phase. The spectra for both samples do not show a well resolved sextet related to Fe atoms on Rh sites, though it should be present. This is probably due to the fact that the peaks are too low to be distinguished above the noise level. The compositional dependence of the hyperfine fields at atoms giving rise to sextet I (0–1 Fe nearest neighbors) agrees very well with the results given in Ref. 23.

The amount of γ phase, obtained from Mössbauer spectroscopy, is plotted in Fig. 8 as a function of the Fe content in the samples. It is clear that the amount of γ phase increases when the Fe content decreases.

D. Saturation magnetization

In Fig. 9 the compositional dependence of the saturation magnetization at 300 K is shown. The results for samples with $x_{\mathrm{Fe}}<0.5$ were obtained after heating the sample to a temperature where the AF→F transition is completed (about 450 K or above) and subsequent cooling to 300 K, where a relatively small field was enough to saturate the magnetization. Samples with $x_{\mathrm{Fe}}>0.5$, which show no magnetic transition, were heated from low temperatures to 300 K. Subsequently a magnetic field was applied that was large enough to saturate the magnetization.

For our thin films with $x_{\mathrm{Fe}}<0.5$ the values can be compared to the values given by Hofer and Cucka for bulk Fe-Rh compounds with excess Rh.[9] The values for these bulk compounds and our thin films compare reasonably well. For $0.5<x_{\mathrm{Fe}}<0.6$ the few experimental results for the saturation magnetization reported in the literature are less systematic (see Table 4 in Ref. 17). Instead of using these data, we calculate the saturation magnetization using the magnetic moments of the Fe and Rh atoms obtained by Shirane *et al.*[19] from neutron diffraction experiments at 298 K. For $0.52<x_{\mathrm{Fe}}<0.6$ they find $m_{\mathrm{Fe}}=3.1\,\mu_B$ and $m_{\mathrm{Fe}}=2.5\,\mu_B$ for Fe atoms on Fe and on Rh sites of the lattice, respectively. The magnetic moment for Rh atoms (on Rh sites) is $m_{\mathrm{Rh}}=1.0\,\mu_B$. The resulting saturation magnetization (dashed line in Fig. 9) compares quite well with our experimental results in this composition range, from which we can conclude that there is no substantial amount of disorder in our films, since disorder would decrease the saturation magnetization.

E. Magnetization and magnetoresistance measurements

Both magnetization and resistance were measured as a function of magnetic field. Before each measurement the films were cooled to 4.2 K and then heated to the desired temperature, so as to create a well defined temperature history. After stabilization at the desired temperature the magnetic field was varied between 0 and 4400 kA/m. In Fig. 10 the magnetization (a) and resistivity (b) loops for a sample with 49.0 at. % Fe at different temperatures are given. The magnetization curves are compensated for the diamagnetic contributions from the substrate and the sample holder. Because of the hysteresis in the magnetization versus temperature loops described earlier, part of the sample is ferromagnetic even at the lowest temperatures. This F fraction is saturated at low fields, as can be seen in Fig. 10(a) for the magnetization curve at 225 K. Increasing the field causes the spins in the AF fraction to rotate over a small angle towards the field direction, resulting in a slow increase of the magnetization and the resistance. At a certain magnetic field there is an upturn in the magnetization curve and the resistance starts to decrease. This is the start of the AF→F transition, and with increasing field the film will become more and more ferromagnetic. At 225 K, far below the transition temperature of this film, the maximum available field of 4400 kA/m is not large enough to have a complete magnetic transition.

Increasing the temperature decreases the magnetic field necessary to start the AF→F transition as can be seen in the resistance versus field curve for 275 K [Fig. 10(b)], where the smallest fields are already enough to start the AF→F transition and to decrease the resistance. At 275 K a MR ratio of $(\rho_0-\rho_{\mathrm{H_{max}}})/\rho_{\mathrm{H_{max}}}=58\%$ is obtained, which is the highest MR ratio we have measured so far in our films. A field of 4400 kA/m is still insufficient to fully saturate the sample at this temperature. At 325 K, a temperature above the transition temperature, the film is mostly ferromagnetic

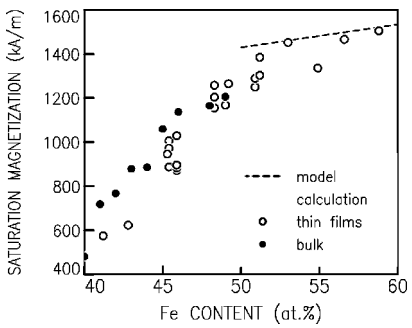

FIG. 9. Measured saturation magnetization for thin films (open circles) compared with the result of a model calculation (dashed line) and experimental values for bulk samples (closed circles), all at 300 K.

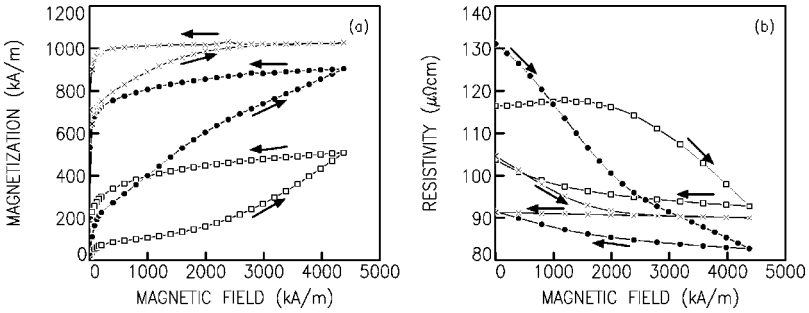

FIG. 10. Magnetization (a) and resistivity (b) as a function of applied magnetic field for a thin film with $x=0.490$ at 225 (□), 275 (●) and 325 K (×). The arrows indicate the direction of the magnetic field change.

even at low fields. The transition is completed at a magnetic field of about 2500 kA/m. Further increase of the magnetic field has almost no effect on magnetization and resistivity. When the magnetic field is decreased again, a large hysteresis is observed for all temperatures, resulting in a larger F fraction after the fieldsweep than before. Other films with different compositions were also investigated and showed the same behavior.

IV. DISCUSSION

A. Compositional dependence of phases observed

The results of our measurements of the compositional dependence of the lattice parameters, the Mössbauer spectrum, and the saturation magnetization of annealed Fe–Rh thin films lead to the following conclusions regarding the occurrence of the various phases around the equiatomic composition:

(1) For $0.51 \leqslant x_{\mathrm{Fe}} < 0.59$ the films are single phase, consisting of the ordered α' phase.
(2) For $0.41 < x_{\mathrm{Fe}} < 0.51$ the films consist of an α'/γ two-phase mixture.

The phase boundary between the single phase α' region and the two-phase α'/γ region is, from the various experimental results obtained, located at $x_{\mathrm{Fe}}=0.505\pm0.015$. The uncertainty is in part the result of the uncertainty in the determination of the composition by RBS (±0.005), but is also related to the measurement accuracies and the sample-to-sample variations observed. From the compositional variation of the saturation magnetization (Fig. 9) the phase boundary between the single phase γ region and the two-phase α'/γ region is estimated to be located at $x_{\mathrm{Fe}}=0.32\pm0.03$.

When comparing these results with the bulk Fe–Rh phase diagram one should remember that the films have been annealed at temperatures up to 970 K, and subsequently cooled with a relatively high rate. Hence, the phases observed are expected to be more closely related to the phase diagram at the temperature of annealing than to the phase diagram at room temperature. We have indicated the boundaries between the single phase and two-phase regions, given above, by arrows in the upper part of the phase diagram presented in Fig. 1. The boundary between the single phase α' region and the two-phase α'/γ region is for our films located at an Fe concentration that is approximately 2 at. % higher than in the bulk phase diagram given by Kubaschewski (Fig. 1, see also Sec. I). On the other hand, in a recent publication Takahashi and Oshima[10] have relocated the phase boundary to the Fe-rich side, varying from $x_{\mathrm{Fe}}\simeq0.52$ for $T=700$ K to $x_{\mathrm{Fe}}\simeq0.51$ for $T=1000$ K. Our results tend to support this latter finding. However, we emphasize that one has to be careful when interpreting thin film results in terms of the phase diagram, in view of the possible occurrence of stress at the temperature of annealing. A discussion of the strain observed in the films is given in part B of this section.

The boundary between the single phase γ region and the two-phase α'/γ region is for our films, within the experimental accuracy, in agreement with the boundary at $x_{\mathrm{Fe}}=0.33$, as given in Fig. 1. Our result is also not significantly different from the results given by Swartzendruber,[17] who has reported a slight temperature dependence of this phase boundary: the boundary is positioned at $x_{\mathrm{Fe}}\simeq0.31$ for $T=700$ K, increasing to $x_{\mathrm{Fe}}\simeq0.35$ for $T=1000$ K.

B. Stress

In Fig. 4 we have presented evidence for the occurrence of tensile stress from the observation of a difference between the in-plane lattice parameter ($a_{\parallel}$) and the perpendicular-to-plane lattice parameter ($a_{\perp}$). In the absence of measurements of the temperature dependence of the strain, we can only present a limited discussion of its origin. Stress can be produced during the growth of the films, and, upon heating the samples, it can result from the phase transformations taking place as well as from a difference between the thermal expansion coefficients of the film and the substrate. However, if the stress that results from these processes is relaxed as a result of annealing during a sufficiently long period of time, the strain observed at room temperature is expected to originate predominantly from the effect of different thermal expansion coefficients of the film and the substrate upon cooling to room temperature.

Assuming that full relaxation has taken place at the annealing temperature, that the strain is homogeneous throughout the film and that there is perfect clamping of the film to the substrate, a first estimate of the strain can be obtained from literature data of the thermal expansion.[15] For the case of cooling from 970 K to room temperature, bulk FeRh shows a linear contraction of approximately 0.54% (neglecting the effect of a possible F→AF transition near room temperature), whereas fused silica glass shows a linear contraction of only approximately 0.04%.[27] At room temperature, $a_{\parallel}$ is then expected to be approximately 0.5% larger than the

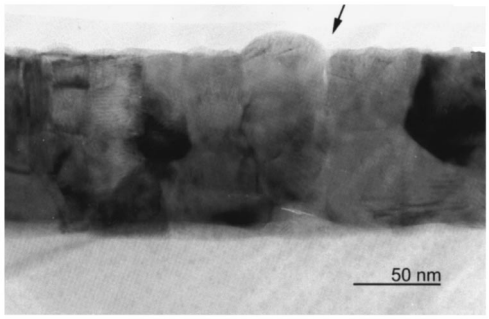

FIG. 11. Cross section TEM image of a film with $x=0.454$, showing a crack at the film surface and evidence of the presence of strain inside the grains.

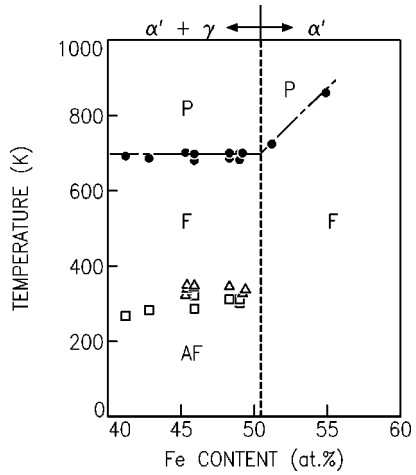

FIG. 12. Compositional dependence of the Curie temperature (●) and the transition temperature of the α' phase in Fe-Rh films for two annealing temperatures, 920 (□) and 970 K (△). The dashed line gives the boundary between the single phase α' region and the two-phase $\alpha'+\gamma$ region at $x_{Fe}=0.505\pm0.015$. Within the experimental accuracy, this line forms also the border line between films that are predominantly AF or completely F at low temperatures.

bulk lattice FeRh parameter. Assuming that the elastic properties of the film are isotropic, it is commonly observed for metals that the change of $a_\perp$ is as large, but of the opposite sign as the change of $a_\parallel$. This would result in a difference between $a_\parallel$ and $a_\perp$ of approximately 1%, and a bulk value of the lattice parameter equal to the average of $a_\parallel$ and $a_\perp$. The experimental values of the lattice parameter difference is smaller, 0.8% for $x_{Fe}<0.49$, decreasing to approximately 0.6% for $x_{Fe}=0.588$ (see Fig. 4). As expected, the bulk lattice parameter (a) is in between $a_\parallel$ and $a_\perp$ for $x_{Fe}>0.49$, although $(a_\parallel-a)$ and $(a_\perp-a)$ are dependent on the composition, and not equal to each other for all compositions investigated. We conclude that the strain observed has the same sign and order of magnitude as expected on the basis of the simplifying assumptions given above, but that these assumptions do not give a fully quantitative description of the observations.

Due to clamping to the substrate the strain will be larger in the region close to the substrate–film interface than in the top of the film. In the top of the film internal stress can relax more easily, especially at grain boundaries, which will cause gaps to appear between grains. A TEM cross-sectional image of a film with $x_{Fe}=0.454$, shown in Fig. 11, provides an indication of the formation of such gaps at the film surface. The resulting relaxation is expected to contribute to the small discrepancy between the calculated and experimental difference of the parallel and perpendicular lattice parameters, discussed above.

C. Dependence of the magnetic transition on composition

The Mössbauer spectra have revealed that all films investigated, consisting of single phase α' phase ($x_{Fe}\geqslant0.505$), are ferromagnetic, whereas in the films consisting of a two-phase α'/γ mixture the α' phase was observed to show at a certain temperature an AF→F transition. A first implication is that in this system single phase FeRh having the α' structure and showing an F→AF transition upon cooling is not present or not resolved experimentally, whereas in contrast, bulk systems of single α' phase showing the F→AF transition are present in an extended compositional range.[10,16,17] A second implication is that for films in the mixed-phase region the composition of the α' phase is independent of the overall film composition, being equal to the composition at the phase boundary. As a result, one expects that, in the absence of effects resulting from microstructural differences and strain, the temperature or (at a fixed temperature) the applied magnetic field at which the magnetic transitions take place are not dependent on the overall film composition.

This conclusion is supported by the observed variation of AF→F transition temperature and of the Curie temperature, with the overall film composition, as shown in Fig. 12. For films annealed at 970 K the transition temperature is 340 ± 10 K, with no significant compositional dependence, whereas for films annealed at 920 K the observed transition temperatures fall in the range of 270–340 K. Although there is a sample-to-sample variation, we again observe no significant compositional dependence. Also the observed Curie temperature is constant in the range of $0.4<x_{Fe}<0.5$.

We cannot exclude the possibility that the tendency of films annealed at 920 K to show a lower transition temperature than that of the films annealed at 970 K results from the combined effect of a slight difference in the composition of the α' phase obtained after annealing at these two temperatures (but still within the range $0.49<x_{Fe}<0.52$) and a strong compositional dependence of the transition temperature. All reports on bulk systems show indeed a strong compositional dependence of the transition temperature.[10,16,17]

A dependence of the final composition on the annealing temperature could be a thermodynamic effect, i.e., due to a dependence of the phase boundary on the temperature, or a kinetic effect, i.e., due to slow diffusion of Rh atoms towards the γ phase precipitates that are formed at the same time.[10] As a result, the Rh concentration across the grains in the film would show a gradient, and the average Rh concentration in the α' phase will slowly decrease. Assuming that the transition temperature is dependent on the Rh concentration, this could then explain the observed wide transition with temperature, and the dependence of the transition temperature on

the annealing temperature. For bulk samples, with much larger grain sizes, an increase of the transition temperature at prolonged annealing is observed.[10] For our thin films, we do not see such an effect, although we cannot exclude that this will be more evident upon employing longer annealing times than we have used so far.

The absence of consensus about the bulk phase diagram and about the compositional dependence of the F to AF transition temperature, presently make it impossible to give a more detailed discussion. A further complication is the possible effect of strain and of the microstructure. This is the subject of the next subsection.

D. Effect on the magnetic transition of strain and microstructure

Whereas for bulk systems the hysteresis in the transition between the F and AF state upon a change of temperature or of the applied field is relatively small,[3,6,7,9] the hysteresis is much larger for thin films. Ohtani and Hatakeyama have already shown that peeling a Fe-Rh film from a SiO_2 substrate causes a decrease of the hysteresis, accompanied by an increase in the transition temperature and a steepening of the magnetic transition.[26] At the same time they observe a tensile stress before peeling (as we have observed in our films) and a volume increase after peeling. The observed decrease of the hysteresis indicates that nucleation and pinning processes depend on strain. The fact that the hysteresis was not completely removed indicates that these processes are in addition related to the occurrence of defects such as, e.g., grain boundaries.

High pressure experiments on bulk systems have shown a decrease of the hysteresis and a decrease of the AF→F transition temperature with increasing pressure.[12,13] From first principles band structure calculations also an increase of transition temperature has been predicted.[21] We note that in a more detailed discussion one has to take into account that both within the experiments and the calculations the lattice remains cubic, whereas in the thin films the lattice is expanded as well as deformed.

Evidence for microstructural effects on the magnetic transition has been reported by Yokoyama *et al.*,[28] who have pointed out that the temperature interval in which the AF→F transition takes place increases with increasing grain size. In our films the grain sizes vary from 10 to 200 nm, affecting the width of the transition, and possibly (as a result of grain-to-grain variations of the strain) the hysteresis.

E. Magnetoresistance ratio

A number of factors are expected to affect the MR ratio of our Fe–Rh thin films. First, the MR ratio depends largely on the microstructure and the composition of the film. For instance, grain boundaries are regions of decreased crystallographic ordering and a source of spin-independent scattering. Since the Fe–Rh compound needs to be almost perfectly ordered to show the magnetic transition it is very likely that the disordered grain boundaries do not contribute to the MR effect. Reduction of the relative contribution of grain boundary scattering to the total resistance by increasing the grain size will then result in a higher MR ratio. Second, for $0.3 < x_{Fe} < 0.51$ part of the film consists of the paramagnetic γ phase, as is shown by Mössbauer spectroscopy, which does not contribute to the change in resistance. The total resistance and therefore also the MR ratio are affected by the resistance of the γ phase and the amount present. Third, the ferromagnetic fraction, which remains even after cooling to the lowest temperatures, does not take part in the magnetic transition. And finally, even at room temperature the maximum available magnetic field of 4400 kA/m is not enough to completely saturate the magnetization, which means that the maximum possible (full) MR ratio cannot be obtained directly. The full MR ratio can be estimated by correcting for the two latter effects as described below.

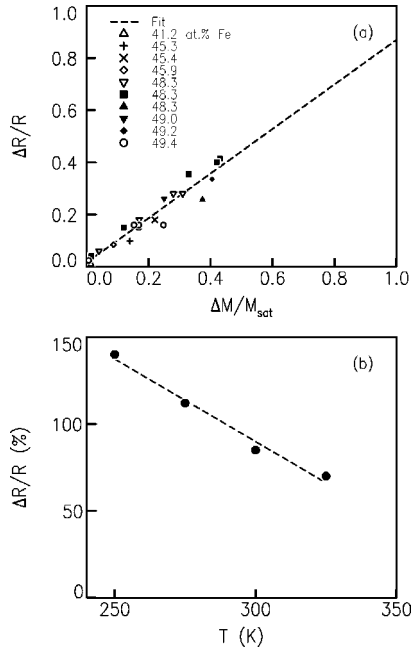

FIG. 13. (a) Magnetoresistance ratio as a function of the relative change of magnetization for several films with different compositions at 300 K. The straight line is a least-squares fit through all data points. At $\Delta M/M_{sat}=1$, $\Delta R/R=85\pm6\%$. (b) The full MR ratio as a function of temperature.

In Fig. 13(a) the MR ratios measured at 300 K are plotted as a function of the relative change of magnetization for several samples with different compositions. The change of magnetization (ΔM) and resistance (ΔR) is determined as the difference between the magnetization and resistance before and after the field sweep to 4400 kA/m, measured at 800 kA/m (see Fig. 10). Hereby the influences of the F and AF fractions as described in Sec. III E are removed. ΔM is divided by the saturation magnetization (M_{sat}) as calculated from the values of the magnetic moments given in Ref. 19 and assuming that there is no γ phase present (see also Sec. III D). To obtain the MR ratio ($\Delta R/R$), ΔR is divided by the lowest resistance for 300 K at $H=4400$ kA/m [see Fig. 10(b)]. However, the resistance at total saturation of the magnetic transition will still be smaller, resulting in a larger $\Delta R/R$. For some samples several data points could be obtained by making use of the temperature hysteresis. For such a purpose the sample was heated first to different temperatures and then cooled down to 300 K. With this method the F

fraction is varied and different magnetization changes and resistance ratios are obtained for the same sample at the same temperature. Before every temperature cycle the sample is cooled down to 4.2 K in zero field to remove all effects from previous temperature or field loops.

A straight line is fitted through all data points and then extrapolated to $\Delta M/M_{\mathrm{sat}}=1$, from which an estimate of the full MR ratio, $\Delta R/R=85\pm6\%$, is obtained. Extrapolation will eliminate the influence of the nonmagnetic γ phase and the insufficient magnetic field on the total magnetization change. The value of $\Delta R/R$ for our films is not significantly different from the value obtained by Algarabel *et al.*, 90% at 295 K for a bulk sample with $x=0.50$.[4] As mentioned before the different amounts of γ phase and the different grain sizes in the films could have an influence on the total resistance and therefore on the MR ratio, but this is not evident from this plot, as data points for various compositions fall on essentially the same line. The same procedure can be followed at other temperatures [see Fig. 13(b)], which shows an increase of the full MR ratio with decreasing temperature. A linear extrapolation gives a full MR ratio of approximately 400% at 0 K. However, we note that there is no physical basis for this linear extrapolation to 0 K, and the temperature interval for which data are available is relatively narrow.

Another way to estimate the full MR ratio at low temperatures is by comparing the resistivities of F ($x_{\mathrm{Fe}}>0.5$) and predominantly AF ($x_{\mathrm{Fe}}<0.5$) samples. We have only used the results from samples with a small amount of γ phase ($0.48<x_{\mathrm{Fe}}<0.5$), in order to almost eliminate a possible influence of the γ phase on the MR ratio. The effect of the low-resistance F fraction in the predominantly AF films is corrected for by plotting the low-temperature resistivity of the samples as a function of the magnetization and extrapolating to zero magnetization (complete antiferromagnetism). Using this method the resistivity of a completely AF sample is found to be 39 ± 5 $\mu\Omega$ cm. The average resistivity for the F samples ($x_{\mathrm{Fe}}>0.5$) is 5 $\mu\Omega$ cm, and a full MR ratio of 680 $\pm100\%$ is obtained at 4.2 K. Schinkel *et al.*[3] obtained MR ratios in bulk samples of 1700% for $x_{\mathrm{Fe}}=0.505$ and 700% for $x_{\mathrm{Fe}}=0.502$ at 4.2 K.

V. CONCLUSIONS

We have shown that there exists a remarkably good agreement between the extrapolated full MR ratio in our thin films and the measured MR ratio in bulk samples, in particular around room temperature. An extrapolation method was used for obtaining the full MR ratio because the films studied generally contain a ferromagnetic fraction that does not contribute to the resistance change. This is caused by a large temperature hysteresis in the magnetic transition. So far we have measured a maximum MR ratio of 58% for a thin film with $x=0.49$ in a magnetic field of 4400 kA/m at 275 K.

The extrapolated full MR ratio does not depend significantly on the alloy composition, within the compositional range studied. This could be explained from the observation from XRD, Mössbauer spectroscopy, and magnetization studies that the composition of the part of the films showing the AF→F transition is independent of the overall Fe content, viz. $x_{\mathrm{Fe}}=0.505\pm0.015$. This is the film composition at the phase boundary between the single phase α' region and the two-phase α'/γ region. Only samples within the two-phase region ($x_{\mathrm{Fe}}<0.505$) show the AF→F transition. No magnetic transition is found for samples with $0.505<x_{\mathrm{Fe}}<0.55$, in contrast to suggestions from bulk phase diagrams.[10,16,17] Although it cannot be ruled out that the occurrence of phases as observed in our Fe–Rh films is influenced by the effect of stress or a certain degree of compositional inhomogeneity, our results certainly suggest that the Fe–Rh phase diagram should be the subject of a future study. Inconsistencies between previously published Fe–Rh phase diagrams, in particular concerning the stoichiometry range in which α' $\mathrm{Fe}_x\mathrm{Rh}_{1-x}$ is, as a single phase, AF at low temperatures, provide an additional motivation for such a study.

There are differences between the magnetic transition in bulk samples and thin films. The magnetic transition in thin films takes place in a wider temperature interval and shows a larger temperature and field hysteresis. These differences can be caused by stress present in the film, possibly showing grain-to-grain variations, or by compositional variations due to different amounts of excess Rh still present in the α' phase due to insufficient annealing times.

In principle, intermetallic compounds such as FeRh showing an AF–F transition that is accompanied by a large magnetoresistance effect could be of interest for applications in magnetic field sensors. A potential advantage of intermetallic compounds with respect to giant magnetoresistance multilayer materials such as exchange biased spin valves is their intrinsic thermal stability. For sensors the use of thin films is highly preferred, making it possible to make use of wafer processing techniques for patterning the material, e.g., in the form of long stripes with a high resistance. However, we presently regard Fe–Rh films as unsuitable for such applications. First, our results confirm the presence of a large thermal and magnetic hysteresis, already reported earlier for thin film structures that were prepared using different methods,[24–26] and we have no indication at present that is possible to decrease this effect substantially. Second, the magnetic fields required for switching at temperatures around room temperature are relatively large [see Fig. 10(b)]. However, our finding that the MR ratio is proportional to the ratio of the magnetization change to the saturation magnetization in the F phase makes it possible to apply Fe–Rh films in studies of the fundamental origin of the MR effect. We are presently exploiting this result in a study of the so-called magnetorefractive effect[29] of Fe–Rh, which is the (wavelength dependent) change of the transmission of infrared light through the films at the AF→F transition.

The observation that the full MR ratio, as obtained for thin films is very close to the value of $\pm90\%$ observed for bulk materials[4] suggests that in these films, and in the bulk samples, the MR effect is due to intrinsic spin-dependent scattering processes (e.g., electron-phonon and electron-magnon scattering). This finding may stimulate first principles calculations of the MR effect at room temperature based on the band structure of perfectly ordered FeRh. First calculations, assuming a spin, configuration (F or AF) and band independent relaxation time have been reported by Go-

mez *et al.*,[30] whose predictions for the MR ratio for diffusive and ballistic transport amount to ± 600 and 400%, respectively. Our results suggest that the difference with the experimental MR ratio at room temperature is unlikely to be due to the neglect of structural disorder.

We find an increase of the full MR ratio from room temperature to 250 K, and (Sec. IV E) a further increase to a full MR ratio of $680 \pm 100\%$ at 4.2 K. As at 4.2 K the effect of defects on the scattering probability is much larger than at room temperature, it is perhaps not very surprising that the latter result is significantly smaller than the bulk value of $\pm 1700\%$ obtained in Ref. 3. In contrast, results for bulk systems displayed in Ref. 4 show an unexpected maximum of the MR ratio of almost 200% around 250 K, below which the MR ratio drops to approximately 85% at 200 K. It would therefore be of much interest to extend the study of the MR ratio of thin film and bulk systems by performing experiments down to 4.2 K in high magnetic fields, of the order 32 MA/m ($B = 40$ T).

ACKNOWLEDGMENTS

The authors would like to thank H.C. Donkersloot, J.M. Kerkhof, E. Janssen, and R.A.F. van der Rijt for their contribution to the sample preparation and W.J.A. De Coster, J.H.M. Snijders, J.J.T.M. Donkers, M.P.C. Krijn, J.L.C. Daams, and P. van der Sluis for helping in the characterization of the samples. This research has been carried out at the Philips Research Laboratories in Eindhoven and has been supported by the Dutch Technology Foundation (STW).

[1] M. N. Baibich, J. M. Broto, A. Fert, F. Nguyen Van Dau, F. Petroff, P. Eitenne, G. Creuzet, A. Friederich, and J. Chazelas, Phys. Rev. Lett. **61**, 2472 (1988).
[2] V. Sechovský, L. Havela, K. Prokeš, H. Nakotte, F. R. de Boer, and E. Brück, J. Appl. Phys. **76**, 6913 (1994).
[3] C. J. Schinkel, R. Hartog, and F. H. A. M. Hochstenbach, J. Phys. F **4**, 1412 (1974).
[4] P. A. Algarabel, M. R. Ibarra, C. Marquina, A. del Moral, J. Galibert, M. Iqbal, and S. Askenazy, Appl. Phys. Lett. **66**, 3062 (1995).
[5] M. R. Ibarra and P. A. Algarabel, Phys. Rev. B **50**, 4196 (1994).
[6] J. S. Kouvel and C. C. Hartelius, J. Appl. Phys. **33**, 1343 (1962).
[7] J. B. McKinnon, D. Melville, and E. W. Lee, J. Phys. C **3**, S46 (1970).
[8] B. K. Ponomarev, Sov. Phys. JETP **36**, 105 (1973).
[9] E. M. Hofer and P. Cucka, J. Phys. Chem. Solids **27**, 1552 (1966).
[10] M. Takahashi and R. Oshima, Mater. Trans., JIM **36**, 735 (1995).
[11] J. M. Lommel and J. S. Kouvel, J. Appl. Phys. **38**, 1263 (1967).
[12] L. I. Vinokurova, A. V. Vlasov, N. I. Kulikov, and M. Pardavi-Horváth, J. Magn. Magn. Mater. **25**, 202 (1981).
[13] R. C. Wayne, Phys. Rev. **170**, 523 (1968).
[14] L. Zsoldos, Phys. Status Solidi **20**, K25 (1967).
[15] C. Marquina, M. R. Ibarra, P. A Algarabel, A. Hernando, P. Crespo, P. Agudo, A. R. Yavari, and E. Navarro, J. Appl. Phys. **81**, 2315 (1997).
[16] O. Kubaschewski, *IRON-Binary Phase Diagrams* (Springer, Berlin, 1982), p. 121.
[17] L. J. Swartzendruber, Bull. Alloy Phase Diagrams **5**, 456 (1984).
[18] F. Bertaut, F. de Bergevin, and G. Roult, Compt. Rendus **256**, 1688 (1963).
[19] G. Shirane, R. Nathans, and C. W. Chen, Phys. Rev. **134**, A1547 (1964).
[20] N. Kunitomi, M. Kohgi, and Y. Nakai, Phys. Lett. A **37**, 333 (1971).
[21] V. L. Moruzzi and P. M. Marcus, Phys. Rev. B **46**, 2864 (1992).
[22] A. Szajek and J. A. Morkowski, J. Magn. Magn. Mater. **115**, 171 (1992).
[23] G. Shirane, C. W. Chen, P. A. Flinn, and R. Nathans, Phys. Rev. **131**, 183 (1963).
[24] J. M. Lommel, J. Appl. Phys. **37**, 1483 (1966).
[25] Y. Ohtani and I. Hatakeyama, J. Appl. Phys. **74**, 3328 (1993).
[26] Y. Ohtani and I. Hatakeyama, J. Magn. Magn. Mater. **131**, 339 (1994).
[27] *Handbook of Materials Science*, edited by C. T. Lynch (Chemical Rubber, Cleveland, 1974), p. 578.
[28] Y. Yokoyama, M. Usukura, S. Yuasa, Y. Suzuki, H. Miyajima, and T. Katayama, J. Magn. Magn. Mater. **177–181**, 181 (1998).
[29] J. C. Jacquet and T. Valet, in *Magnetic Ultrathin Films, Multilayers and Surfaces*, edited by E. E. Marinero *et al.*, MRS Symposia Proceedings No. 384 (Materials Research Society, Pittsburgh, 1995), p. 477.
[30] R. Gómez Abal, A. M. Llois, and M. Weissmann, Phys. Rev. B **53**, R8844 (1996).